Available online at www.sciencedirect.com
ScienceDirect
Trans. Nonferrous Met. Soc. China 20(2010) 675−681
Transactions of Nonferrous Metals Society of China
www.tnmsc.cn

Microscopic phase-field study on aging behavior of $Ni_{75}Al_{17}Zn_8$ alloy

ZHAO Yan(赵 彦)[1], CHEN Zheng(陈 铮)[1, 2], LU Yan-li(卢艳丽)[1], ZHANG Li-peng(张利鹏)[1]

1. College of Materials Science and Engineering, Northwestern Polytechnical University, Xi'an 710072, China;
2. State Key Laboratory of Solidification Processing, Northwestern Polytechnical University, Xi'an 710072, China

Received 22 December 2008; accepted 4 May 2009

Abstract: The precipitating kinetics of $Ni_{75}Al_{17}Zn_8$ alloy was studied at both 873K and 973K by microscopic phase-field model. The calculation results show that the order−disorder transformation experiences the matrix → lowly-ordered $L1_0$ phase → $L1_2$ phase at 973 K. And the nucleation of $L1_2$ particles belongs to the spinodal decomposition mechanism. As temperature increases, orderings of Al and Zn atoms are resisted, but coarsening of $L1_2$ particles is promoted. The value of coarsening kinetic exponents approaches to 1/2. In addition, the discussions about Ni-Al anti-site defect and Zn substitutions for Ni site and Al site exhibit that the higher the temperature, the more distinctive the Ni-Al anti-site defect, but the less the Zn substitution.
Key words: microscopic phase-field; $Ni_{75}Al_{17}Zn_8$ alloy; coarsening behavior

1 Introduction

The Ni_3Al intermetallic compound with $L1_2$ structure has attracted considerable interests as the monolithic high temperature structural material and as a component in composite because of its positive temperature dependence of the yield strength[1]. Especially for matrix→$L1_2$ order−disorder structural transformation, experiments and theoretical studies have involved every stage in this process, such as nucleation mechanism[2−3], coarsening behaviors[4−5] and mechanical performance. As computer simulations were brought in, more and more approaches have been established for explaining its phase transformation mechanism and material behaviors.

Phase-field model is one of the available methods for calculating metallic isothermal process. Based on this model, CHEN et al[2, 6] discussed about the nucleation mechanisms of Ni-Al-V and Ni-Al-Cr alloys, which displayed the transition from spinodal decomposition mechanism to nucleation and growth mechanism in a special composition range.

For coarsening behaviors during precipitation, common analysis lies in the size of particles satisfying exponent relationship with time, and dynamic scaling regulation, which are associated with TEM observation and small-angle neutron scattering experiment[7]. Based on the description of conserved and non-conserved field variables, the kinetic exponent (n) takes on different values. For the conserved field variable parameter, n= 1/3; for the non-conserved field variable parameter, n=1/2; and for the conserved vector order parameter, n=1/4. Nevertheless, using Monte Carlo simulation method, PAREIGE et al[8] proved that the coarsening procedure could be divided into two stages with different exponents. The similar results were else required by microscopic phase-field modeling. MIYAZAKI et al[9] explained this behavior as the influence of volume fraction and elastic energy.

Atomic occupation in Ni-Al alloy has taken attention of researchers because of the existence of Ni-Al anti-site defect and the influence of the third element on mechanical performances. RAWLING and STATON-BEVAN[10] studied the relationship between the mechanical properties and site preferences of the third element in $\gamma'(Ni_3Al)$ phase, and concluded that in order to enhance yield strength, the ternary additions should substitute Al site. According to the studies about Ni-Al anti-site defect[11−13] and Zn substitution[14] in γ' phase, Zn preferred to occupy Al site.

Most of these studies were based on the method of atomic short-range interactions. In contrast with the short range order (SRO) method, microscopic phase field

Foundation item: Projects(50941020, 10902086) supported by the National Natural Science Foundation of China
Corresponding author: ZHAO Yan; Tel: +86-29-88474095; E-mail: zhaoyan8626@126.com
DOI: 10.1016/S1003-6326(09)60197-7

model belongs to long range order (LRO) method[15] and has the advantage with the visible graphic expression of atomic occupation probabilities.

In this work, microscopic phase-field method is applied to study isothermal aging process of $Ni_{75}Al_{17}Zn_8$ alloy, including nucleation mechanism, coarsening kinetic etc. Meanwhile, the simulated results are compared with the experimental results.

2 Theoretical model

The phase-field dynamic equation is founded based on the Onsager and Ginzburg-Landau theory, which describes the atomic configuration and precipitation pattern of the ordered phases by occupation probability $P(\boldsymbol{r}, t)$ at lattice site $\boldsymbol{r}$ and time t. The microscopic kinetic equation (TDGL equation) is written as

$$\frac{\partial P(\boldsymbol{r},t)}{\partial t}=\sum_{\boldsymbol{r}'}L(\boldsymbol{r}-\boldsymbol{r}')\frac{\delta F}{\delta P(\boldsymbol{r}',t)} \tag{1}$$

In the mean-field approximation[15], the free energy for ternary system is given by

$$\begin{aligned}F=&-\frac{1}{2}\sum_{\boldsymbol{r}}\sum_{\boldsymbol{r}'}\big[(-V_{\mathrm{AB}}(\boldsymbol{r}-\boldsymbol{r}')+V_{\mathrm{BC}}(\boldsymbol{r}-\boldsymbol{r}')+\\&V_{\mathrm{AC}}(\boldsymbol{r}-\boldsymbol{r}'))P_{\mathrm{A}}(\boldsymbol{r})P_{\mathrm{B}}(\boldsymbol{r}')+V_{\mathrm{AC}}(\boldsymbol{r}-\boldsymbol{r}')P_{\mathrm{A}}(\boldsymbol{r})P_{\mathrm{A}}(\boldsymbol{r}')+\\&V_{\mathrm{BC}}(\boldsymbol{r}-\boldsymbol{r}')P_{\mathrm{B}}(\boldsymbol{r})P_{\mathrm{B}}(\boldsymbol{r}')\big]+\\&k_{\mathrm{B}}T\sum_{\boldsymbol{r}'}\big[P_{\mathrm{A}}(\boldsymbol{r})\ln(P_{\mathrm{A}}(\boldsymbol{r}))+P_{\mathrm{B}}(\boldsymbol{r})\ln(P_{\mathrm{B}}(\boldsymbol{r}))+\\&(1-P_{\mathrm{A}}(\boldsymbol{r})-P_{\mathrm{B}}(\boldsymbol{r}))\ln(1-P_{\mathrm{A}}(\boldsymbol{r})-P_{\mathrm{B}}(\boldsymbol{r}))\big]\end{aligned} \tag{2}$$

where the first sum represents the chemical energy, and the second sum is the thermal dynamic energy in this system; k_{B} is the Boltzmann constant; $V_{\alpha\beta}(\boldsymbol{r}-\boldsymbol{r}')$ is the effective interactive energy given as the sum of the α—α, β—β pairwise interactive energies, minus twice the α—β pairwise interactive energy:

$$V_{\alpha\beta}(\boldsymbol{r}-\boldsymbol{r}')=W_{\alpha\alpha}(\boldsymbol{r}-\boldsymbol{r}')+W_{\beta\beta}(\boldsymbol{r}-\boldsymbol{r}')-2W_{\alpha\beta}(\boldsymbol{r}-\boldsymbol{r}') \tag{3}$$

In this model, four nearest-neighborhood interactions are entitled in the approximation of atomic interactions. $V_{\alpha\beta}^{1}$, $V_{\alpha\beta}^{2}$, $V_{\alpha\beta}^{3}$, $V_{\alpha\beta}^{4}$ denote the first-nearest, second-nearest, third-nearest and fourth-nearest interactive potentials, respectively, then they are introduced into the FCC lattice. Here, $W_{\alpha\alpha}$, $W_{\beta\beta}$ and $W_{\alpha\beta}$ stand for the pairwise potentials between α—α, β—β, and α—β, respectively. For reciprocal space, there is

$$\begin{aligned}V_{\alpha\beta}(\boldsymbol{k})=&4V_{\alpha\beta}^{1}(\cos\pi h\cdot\cos\pi k+\cos\pi h\cdot\cos\pi l+\cos\pi k\cdot\\&\cos\pi l)+2V_{\alpha\beta}^{2}(\cos 2\pi h+\cos 2\pi k+\cos 2\pi l)+\\&8V_{\alpha\beta}^{3}(\cos 2\pi h\cdot\cos\pi k\cdot\cos\pi l+\cos\pi h\cdot\cos 2\pi k\cdot\\&\cos\pi l+\cos\pi h\cdot\cos\pi k\cdot\cos 2\pi l+4V_{\alpha\beta}^{4}(\cos 2\pi h\cdot\\&\cos 2\pi k+\cos 2\pi h\cdot\cos 2\pi l+\cos 2\pi k\cdot\cos 2\pi l)\end{aligned} \tag{4}$$

where k, h and l represent the reciprocal lattice site through

$$\boldsymbol{k}=(k_x,k_y,k_z)=h\boldsymbol{a}_1^*+k\boldsymbol{a}_2^*+l\boldsymbol{a}_3^* \tag{5}$$

with $\boldsymbol{a}_1^*$, $\boldsymbol{a}_2^*$, $\boldsymbol{a}_3^*$ being the unit reciprocal lattice vectors of the FCC structure along [100], [010] and [001] directions.

Referring to the results of MEKHRABOV et al[14], the atomic ordering energy of Ni-Al-Zn alloy is acquired, as shown in Fig.1, where $W(R)=-0.5V(R)$ and R_1, R_2, R_3 represent the first, second and third nearest-neighborhood interatomic distances with defining $W(R_4)=0$.

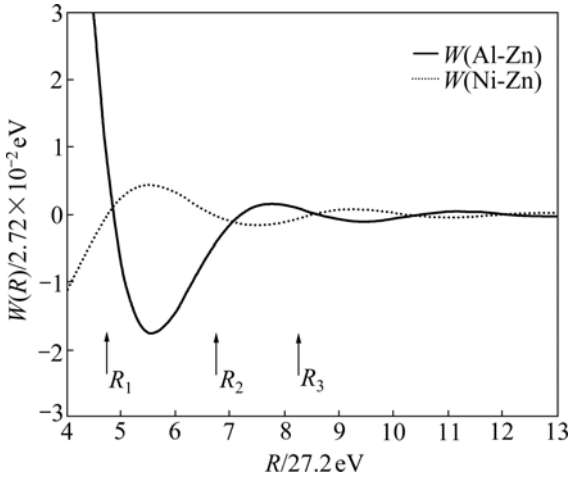

Fig.1 Variation of ordering energies with interatomic distance calculated by pseudopotential approximation[14]

3 Simulation results and analysis

3.1 Nucleation mechanism of γ' phase

Projecting 3D crystal structure to 2D images along [001] direction, Fig.2 shows three kinds of crystalline structures, that is, disordered matrix (γ phase), $L1_2$ (γ' phase) and $L1_0$. In addition, $L1_2$ structure is classified into α site (Ni site) and β site (Al site), corresponding to the center site and the corner site in FCC structure, respectively.

By solving TDGL equation, the node values of 128×128 matrix are got. With time steps increasing, system evolving is obtained. In matrix, lattice gray level represents the occupational probabilities of Ni at every lattice node. The higher the Ni occupation is, the brighter the gray level of nodes is.

Fig.3 shows the temporal evolutions of atomic images at both 873 K and 973 K. It can be seen that, the ordering at 873 K proceeds faster than that at 973 K. γ' particles precipitate from the matrix at the 3 600th step

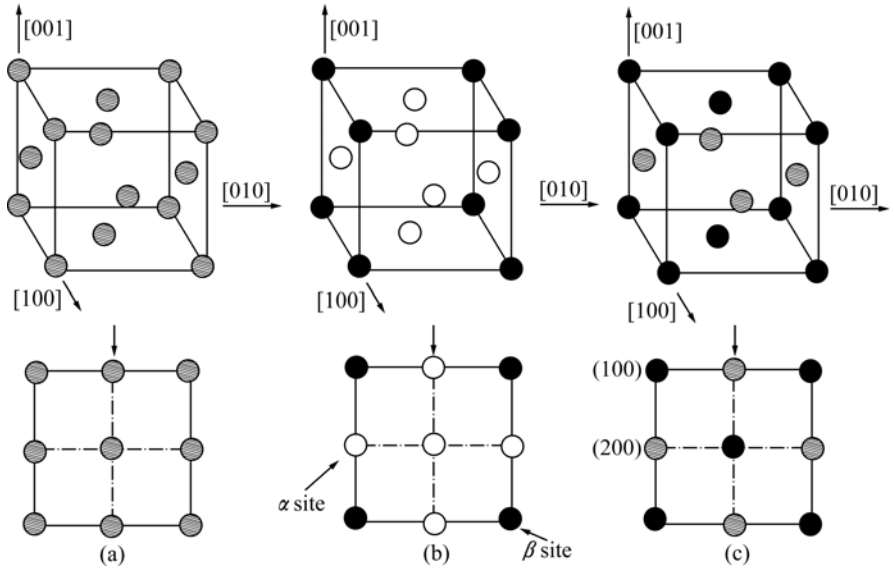

Fig.2 3D lattice structures and their 2D projection along [001] direction: (a) γ phase; (b) $L1_2$ structure; (c) $L1_0$ structure

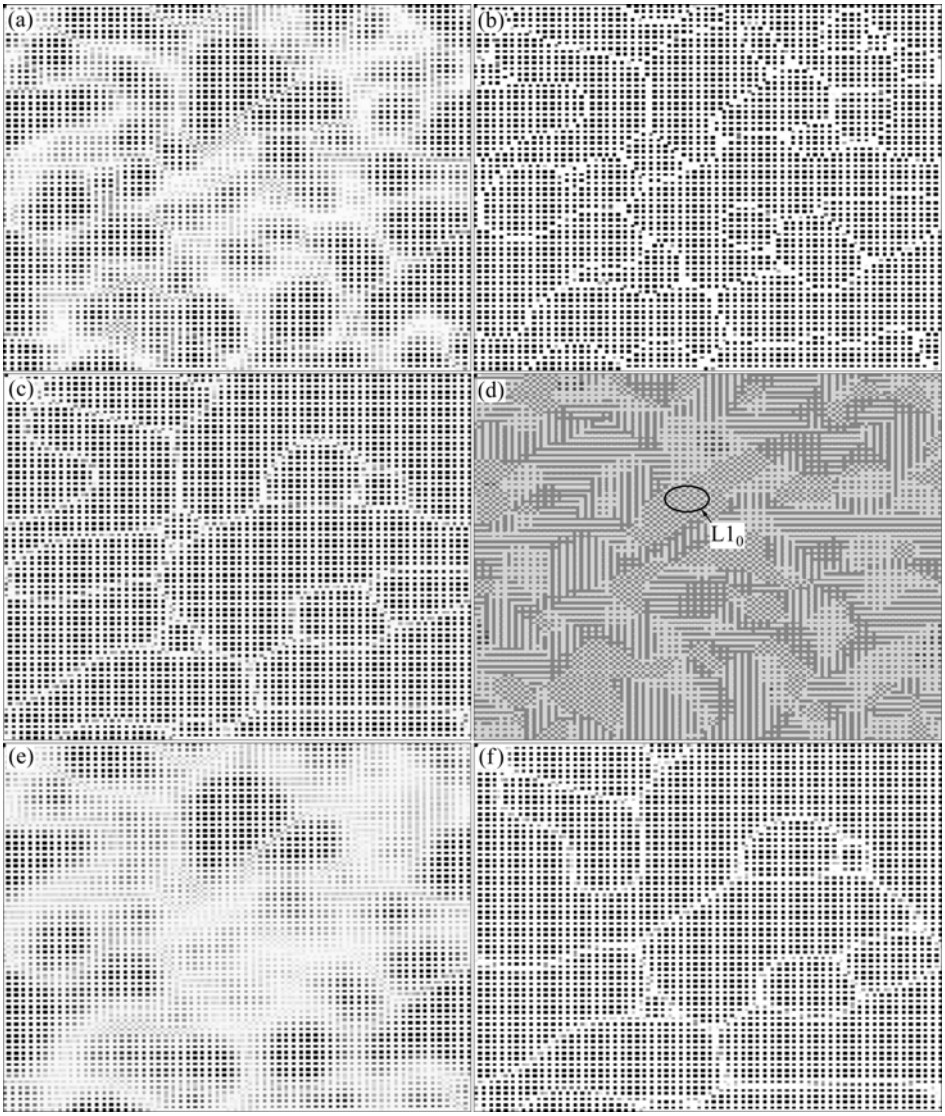

Fig.3 Temporal evolution of atomic images in aging process of $Ni_{75}Al_{17}Zn_8$ alloy by microscopic phase-field modeling: (a) T=873 K, t=3 600th step; (b) T=873 K, t=6 400th step; (c) T=873 K, t=20 000th step; (d) T=973 K, t=3 600th step; (e) T=973 K, t=6 400th step; (f) T=973 K, t=20 000th step

during 873 K aging; while intermediate $L1_0$ phase with lower ordering degree is firstly produced, then $L1_0 \rightarrow L1_2$ transformation happens at the 6 400th step in 973 K aging. At this time step, the precipitated γ' particles at 873 K aging are close to each other and grow into coarsening stage. After the growth and coarsening stage the morphologies go to the final phase, as shown at the 20 000th step.

According to atomic images, there are two types of ordering mechanisms: direct ordering mechanism at 873 K and indirect ordering mechanism at 973 K. The direct ordering mechanism does not involve the transition of the intermediate phase, but matrix$\rightarrow L1_2$ transformation straightly. The indirect ordering mechanism has two stages in transformation as follows. In stage Ⅰ, the low-ordered $L1_0$ phase forms at first with characterized atomic ordering on (100) and (200) lattice face simultaneously. And in stage Ⅱ, $L1_1$ phase is precipitated in the process of $L1_0 \rightarrow L1_2$ transformation. Al and Zn atoms are concentrated and ordered on (100) face.

The calculation results can be compared with 3DAP experiment and Monte Carlo simulation in Ni-Al-Cr alloy by PAREIGE et al[8]. It was similar to this work in the aspect that the ordering on (100) face is firstly observed before the formation of $L1_2$ phase.

For the better description of atomic ordering, an ordering parameter is introduced as a measurement. According to Khachturyan's theory, the formula can be written as

$$\eta(i, j) = \frac{P(i, j) - C(i, j)}{C(i, j) \cdot \cos\pi(i + j)} \tag{6}$$

where $\eta(i, j)$ is called the long range ordering (LRO) parameter whose value can be used to express the atomic ordering level at site (i, j); $P(i, j)$ stands for the atomic occupation probability at site (i, j); and $C(i, j)$ denotes the average occupation probability.

Fig.4 shows the temporal evolution of LRO parameter of Al and Zn atoms across the diameter of one particle during aging. It could be seen that, the nucleation of particle experiences the increase of the LRO parameter, which corresponds to the growth of $L1_2$ phase particle. Then, it continues to grow along radius direction. Finally, it arrives at equilibrium. But the final values of LRO parameter of Al and Zn are not equal. The final LRO parameter of Al approaches to 1, which is higher than that of Zn (close to 0.6). Noticing the discrepancy of the LRO parameters at different temperatures, the elevation of temperature is unfavorable to enhancing the final equilibrium of Al and Zn ordering degree. The

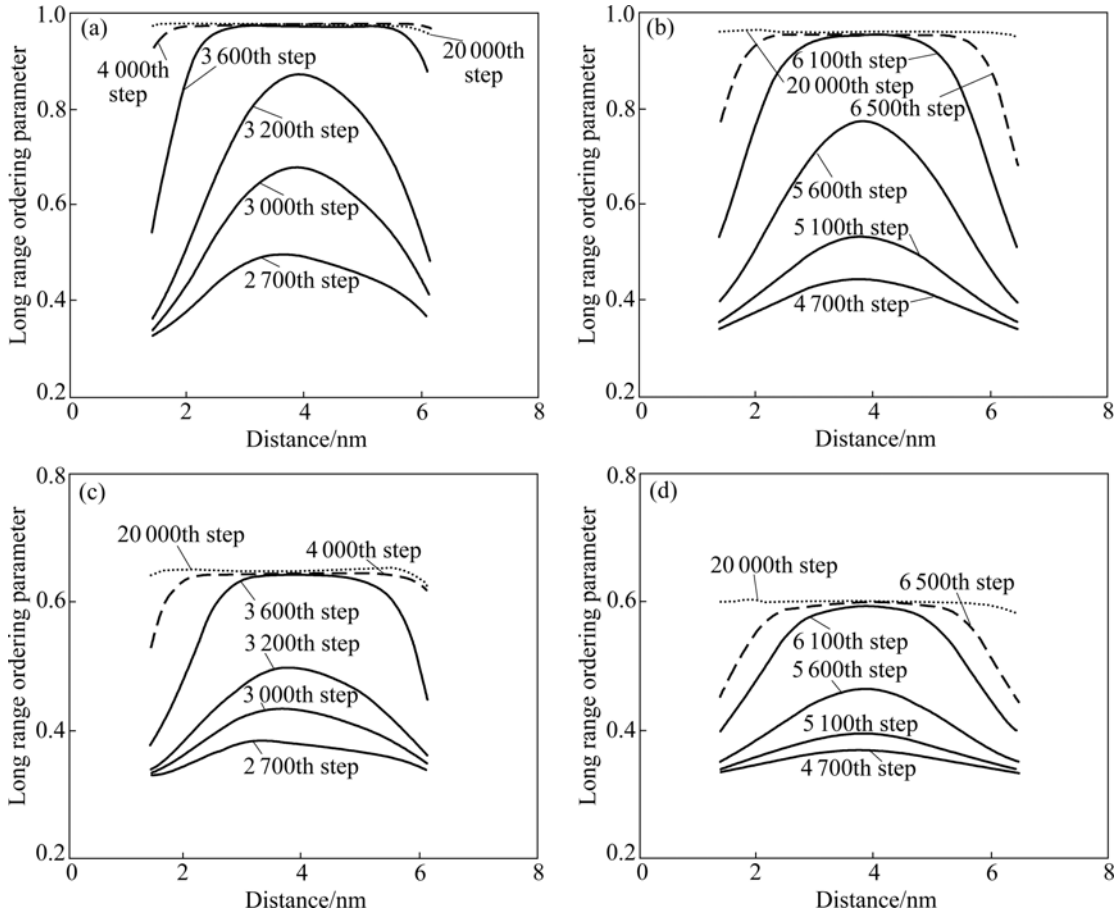

Fig.4 Temporal evolution of long range ordering parameter of Al((a) and (b)) and Zn((c) and (d)): (a) and (c) T=873 K; (b) and (d) T=973 K

calculated value of Al at 873 K is equal to 0.97, greater than 0.95 at 973 K; similarly, that of Zn is equal to 0.67 at 873 K, greater than 0.60 at 973 K. It is demonstrated that increasing the temperature resists atomic ordering.

In the previous investigation, the studies of lowly supersaturated alloys confirmed that the nucleation of ordered particles was supposed to follow a nucleation and growth mechanism. For highly supersaturated alloys, congruent ordering was expected to happen before phase separation. In this system, from the calculation results, the nucleation satisfies the spinodal decomposition mechanism with characteristics of "wide scope, small fluctuation", described by the fundamental phase transformation theory.

3.2 Coarsening kinetics of γ' phase

The coarsening kinetics of γ' phase in Ni-Al alloys were investigated with the methods of both experiments and computer simulations[4, 16]. The common ways of analysis focus on the descriptions of the kinetic exponent as well as the dynamic scaling (involved in structural self-similarity)[16, 17], which depend on the dynamic properties of valuables, including interface migration and atomic diffusion.

In Fig.5 the temporal evolution of the quantity and average diameter of $L1_2$ phase particles at 873 K and 973 K is plotted. The change of particles number and average diameter experiences three stages. At the beginning of aging, as no particle is precipitated from matrix, there is none of changes. By then, $L1_2$ phase particles go into the nucleation and growth stage where the particles number and size increase sharply. When particles grow big enough and are close to each other, the coalescence among them takes place. During this coarsening stage, particle number reduces but its average diameter increases. Compared with the earlier evolution, the growth of particles in coarsening stage becomes smooth.

Here, we introduce coarsening kinetic exponent to investigate the coarsening kinetics of $L1_2$ phase, which could be helpful to reflecting the time dependence of particle growth. By solving Cahn-Hilliard or Ginzburg-Landau equations, the influence of composition field variables and ordering parameter field variables on kinetic exponent was exhibited[4]. Yet, Monte Carlo simulation proved that the value of kinetic exponent n approximated to 1/2 in the beginning, but then, turned into 1/3 with the drop of supersaturation in $L1_2$ phase.

Considering the relationship between average diameter and time, the average diameter D of particles obeys $D=k\cdot t^n$, where k is a coefficient and t represents time. In this simulation, n=1/2, which was confirmed by Monte Carlo simulation elsewhere[8]. In addition, it can also be seen that with temperature increasing, the coarsening stage is lagged; but whatever the temperature is, the kinetic exponent maintains the same value (as shown in Fig.5).

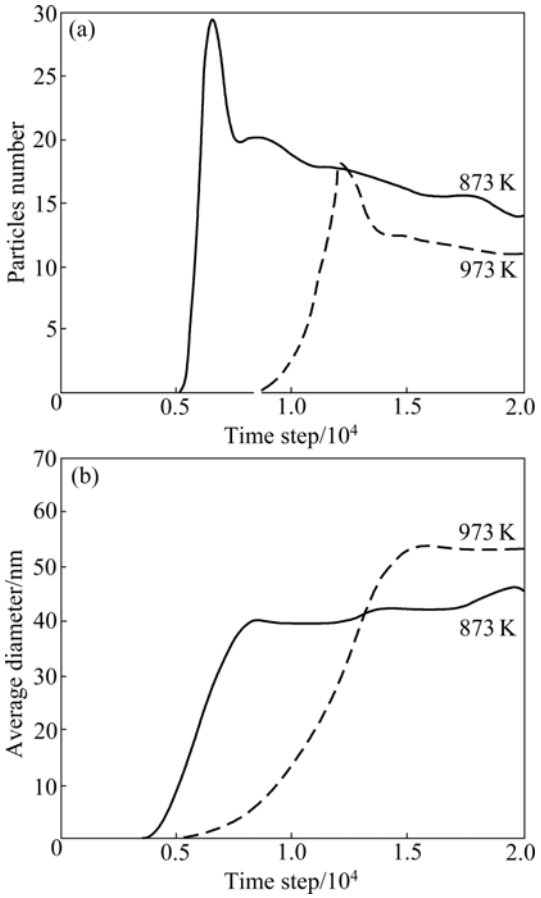

Fig.5 Temporal evolution of particles number (a) and average diameter (b) of $L1_2$ phase

3.3 Ni-Al anti-site and Zn substitution

According to previous experiments and theoretical analysis, atomic occupation features were studied and identified that Zn tends to substitute Al site, and meanwhile, the Ni-Al anti-site defect has great effect on the mechanical performances.

In computer simulations, short range ordering (SRO) method is more widely used to discuss structural stabilities and dynamic behaviors, which is helpful to understanding its essential physical reasons. As LRO method is built up, atomic occupation probabilities are brought into the discussion of atoms behavior by statistics methods. In this work, the calculation results using LRO method are discussed.

Fig.6 shows the temporal evolution of the occupation probability of elements Ni, Al and Zn at α and β sites. At first, element occupations at lattice site are laid on the initial values. Subsequently, elements are chosen to occupy their own sites. Al prefers to occupy β

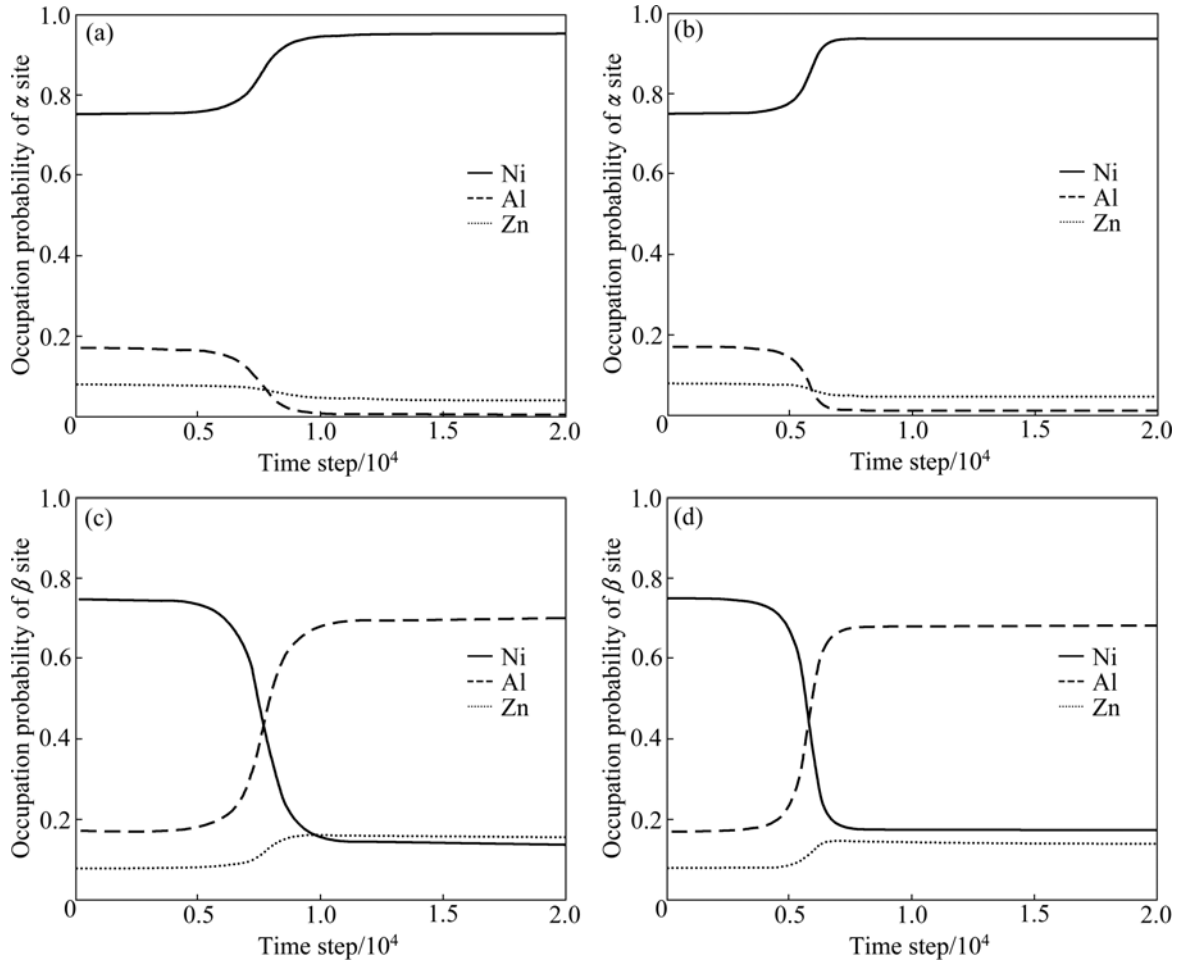

Fig.6 Temporal evolutions of occupation probabilities of Ni, Al, and Zn atoms during aging: (a) α site, T=873 K; (b) α site, T=973 K; (c) β site, T=873 K; (d) β site, T=973 K

site (Al site), with a bit occupying of α site (Ni site) and anti-site Ni site. Ni atoms have similar behaviors, to occupy α site (Ni site) and Al anti-site. Moreover, the tendency of Al anti-site of Ni is more obvious than that of Ni anti-site of Al. This is in good agreement with the experimental and calculated results that when x(Ni):x(Al)>3:1, the tendency of Al anti-site of Ni in γ' phase becomes intensified.

As the third component, Zn occupies both sites and has a tendency of substituting Al site, which was demonstrated by some works mentioned above[14]. According to this study, Zn concurs to substitute both Al and Ni sites, but tends to occupy Al site dominantly.

Considering the influences of temperature, it could be found that with temperature increasing, the extent of Ni-Al anti-site is strengthened, and Zn substitution is decreased. It is simply explained that temperature rising activates the diffusion of atoms, which provides more formation energy of defects. With the hybrid entropy decreasing, the ordering degree of $L1_2$ phase becomes low. The anti-site defect is adaptable to form. Nevertheless, Zn prefers to precipitate from $L1_2$ phase.

4 Conclusions

1) When aging at 973 K, lowly-ordered $L1_0$ phase is formed firstly. And the ordering degree of alloy elements decreases with temperature increasing.

2) The nucleation mechanism of $L1_2$ phase is identified to be the spinodal decomposition at both 873 K and 973 K. The coarsening kinetic exponent of particles approaches to 1/2. The rising of temperature promotes the coalescence of particles.

3) The ratio of Al anti-site of Ni is greater than that of Ni anti-site of Al in aging at both 873 K and 973 K. With the increase of temperature, Ni-Al anti-site defects become obvious, but the substitutions of Zn for Ni and Al become little.

References

[1] FISCHER R, ELENO L T F, FROMMEYER G, SCHNEIDER A. Precipitation of Cr-rich phases in a Ni-50Al-2Cr(at.%) alloy [J]. Intermetallics, 2006, 14(2): 156−162.

[2] LI Y S, CHEN Z, LU Y L, WANG Y X, ZHANG J J. Computer

simulation of the precipitation process of $Ni_{75}Al_{7.5}V_{17.5}$ alloy [J]. Progress in Natural Science, 2004, 14(12): 1099−1104.

[3] LI Yong-sheng, CHEN Zheng, LU Yan-li, WANG Yong-xin. Phase-field simulation of phase separation in $Ni_{75}Al_xV_{25-x}$ alloy with elastic stress [J]. Transactions of Nonferrous Metals Society of China, 2006, 16(s3): 2017−2021.

[4] ZHU J Z, WANG T, ARDELL A J, ZHOU S H, LIU Z K, CHEN L Q. Three-dimensional phase-field simulations of coarsening kinetics of γ' particles in binary Ni-Al alloys [J]. Acta Mater, 2004, 52(9): 2837−2845.

[5] LAPIN J, VANO A. Coarsening kinetics of α- and γ'-precipitates in a multiphase intermetallic Ni-Al-Cr-Ti type alloy with additions of Mo and Zr [J]. Scripta Materialia, 2004, 50(5): 571−575.

[6] CHU Z, CHEN Z, WANG Y X, LU Y L, LI Y S. Atomic-scale computer simulation for ternary alloy Ni-Cr-Al during early precipitation process [J]. Progress in Natural Science, 2005, 15(7): 656−660.

[7] LIU Jun-ming, WU Zhuang-chun, LIU Z G. Dynamic scaling of phase separation in amorphous $Cu_{12.5}Zr_{41}Ti_{14}Be_{22.5}$ alloy [J]. Acta Physica Sinica, 1997, 46(6): 1146−1152. (in Chinese)

[8] PAREIGE C, SOISSON F, BLAVETTE D. Ordering and phase separation in low supersaturated Ni-Cr-Al alloys: 3D atom probe and Monte Carlo simulation [J]. Materials Science and Engineering A, 1998, 250(1): 99−103.

[9] MIYAZAKI T, KOYAMA T, KOZAKAI T. Computer simulation of the phase transformation in real alloy systems based on the phase field method [J]. Materials Science and Engineering A, 2001, 312(1/5): 38−49.

[10] RAWLING R D, STATON-BEVAN A E. The alloying behavior and mechanical properties of polycrystalline $Ni_3Al(\gamma'$ phase) with ternary additions [J]. Mater Sci, 1975, 10: 505−514.

[11] HAO Y L, YANG R, SONG Y, CUI Y Y, LI D, NIINOMI M. Concentration of point defects and site occupancy behavior in ternary NiAl alloy [J]. Material Science and Engineering A, 2004, 365(1/2): 85−89.

[12] SCHWEIGER H, SEMENOVA O, WOLF W, PÜSCHL W, PFEILEI W, PODLOUCKY R, IPSER H. Energetics of point defect formation in Ni_3Al [J]. Scripta Materialia, 2002, 46(1): 37−41.

[13] JIANG C, GLEESON B. Effect of Cr on the elastic properties of B2 NiAl: A first-principles study [J]. Scripta Materialia, 2006, 55(9): 759−762.

[14] MEKHRABOV A O, VDENIZ M V, ARER M M. Atomic ordering characteristics of Ni_3Al intermetallics with substitutional ternary additions [J]. Acta Mater, 1997, 45(3): 1077−1083.

[15] PODURI R, CHEN L Q. Computer simulation of the kinetics of order-disorder and phase separation during precipitation of δ' (Al_3Li) in Al-Li alloys [J]. Acta Mater, 1997, 45(1): 245−255.

[16] MAEBASHI T, DOI M. Coarsening behaviours of coherent γ' and γ precipitates in elastically constrained Ni-Al-Ti alloys [J]. Materials Science and Engineering A, 2004, 373(1/2): 72−79.

[17] MENON G. Mathematical approaches to dynamic scaling [J]. J Non-Newtonian Fluid Mech, 2008, 152(1/3): 113−119.

(Edited by YANG Bing)